Chapter 3
Dynamic Electro-, Mechanochromic Materials and Structures for Multifunctional Smart Windows

Yao Zhao, Yanbin Li, and Jie Yin

Abstract As one of the key elements in building envelopes, smart windows that can adaptively block and transmit sunlight for energy saving are promising to construct energy-efficient buildings and reduce the greenhouse gas emissions. Most smart windows are based on electro-, thermo-, mechano-, and photochromics for single-purpose, passive energy saving. Considering the large surface area of windows in modern buildings, recent research advances witness the demand of embodying multifunctionality in smart windows for integrating additional beneficial functions, including energy storage and self-powering, self-cleaning, and even water harvesting to tackle the water scarcity challenge. These multifunctionality requires redesigning conventional smart windows in terms of new materials selection and synthesis, device fabrication, surface features, and structural designs. In this chapter, we will briefly discuss the recent advances in multifunctional smart windows, including harnessing electrochromism and thermochromism for energy storage and generation alongside integrated perovskite solar cells, surface wetting for self-cleaning, and combined wetting and optical properties in novel wrinkling and kirigami structures for water harvesting. The involved materials synthesis, device fabrication, characterization, mechanisms, and multifunctional performances are discussed. We hope it can provide constructive insights for designing next-generation multifunctional smart windows to make buildings more energy efficient and environmentally sustainable.

Keywords Multifunctional smart windows · Energy storage · Self-powering · Self-cleaning · Water harvesting · Wrinkling · Kirigami

Y. Zhao · Y. Li · J. Yin (✉)
Department of Mechanical and Aerospace Engineering, North Carolina State University, Raleigh, NC 27695, USA
e-mail: jyin8@ncsu.edu

Y. Zhao
e-mail: yzhao59@ncsu.edu

Y. Li
e-mail: yli255@ncsu.edu

J. Wang et al. (eds.), *Advanced Materials in Smart Building Skins for Sustainability*,
https://doi.org/10.1007/978-3-031-09695-2_3

3.1 Introduction

To date, buildings account for 30% of the global energy consumption (Isaac & van Vuuren, 2009; Pérez-Lombard et al., 2008; Vieira et al., 2019) To meet the 2050 Carbon Neutrality mission (Guterres, 2020; EU, 2020; DOE, 2021) advocated by United Nations, energy-efficient buildings are highly demanded to save energy and reduce the greenhouse gas emissions (Piccolo & Simone, 2015). Smart windows, as one of the key elements in building envelopes, can modulate the light transmittance into the buildings for reducing the electrical, cooling or heating energy consumptions for energy saving (Bechinger et al., 1996; Granqvist, 2000; Casini, 2018; Wang et al., 2019b). They can block the sunlight with low transmittance in hot and shiny days to maintain cool indoor environment and keep warm with high transmittance during cold days. By tuning solar irradiation and/or radiative cooling, it can effectively reduce the burden of heating, ventilation and air conditioning (HVAC) that account for about 50% of building energy consumption (Ke et al., 2018; Pérez-Lombard et al., 2008). Thus, smart window is one of the ideal candidates to reduce the building energy consumption (Dussault et al., 2012; Parkin & Manning, 2006; Wang et al., 2016b; Zhang et al., 2020).

Current state-of-the-art smart windows can be generally classified into four categories in terms of the working mechanisms for modulating the optical transmittance: thermochromic (Aburas et al., 2019; Kamalisarvestani et al., 2013), electrochromic (Azens & Granqvist, 2003; Macêdo et al., 1992), photochromic (Tällberg et al., 2019), and mechanochromic (Ge et al., 2015; Lin et al., 2017). Correspondingly, their optical transmittance can be tuned by means of temperature (Aburas et al., 2019; Kamalisarvestani et al., 2013), electric potentials (Azens & Granqvist, 2003; Macêdo et al., 1992), light intensity or light wavelengths (Chun et al., 2021; Tällberg et al., 2019; Wang et al., 2019a), and mechanical deformations (Ge et al., 2015; Lin et al., 2017). However, these smart windows are often designed for the single functionality of blocking or letting through sun light for passive energy saving.

Considering the large surface area of windows or façade in modern buildings, how to integrate large-area surface structures and novel materials for embodying multifunctionality into smart windows has recently attracted growing research interest. In addition to the energy saving, some representative strategies for achieving multifunctional performances include energy harvesting and energy storage, electricity generation for self-powering, surface wettability for self-cleaning, and water harvesting from environments for addressing the water scarcity issue in draught areas. In this chapter, we will focus on energy-efficient smart windows with such novel multifunctionalities, including energy storage (Sect. 3.2.1), electricity generation (Sect. 3.2.2), self-cleaning (Sect. 3.2.3), and water harvesting (Sect. 3.2.4). Materials synthesis, device fabrication, and some key features of these smart windows will be discussed based on several representative works. Lastly, perspectives for future developments are discussed in Sect. 3.3.

3.2 Multifunctional Smart Windows

3.2.1 Combined Energy Saving and Energy Storage

In addition to tuning optical transmittance for better indoor thermal management, smart windows are also desired to be energy-saving effectively (Baetens et al., 2010; Cai et al., 2016; Casini, 2018; Cao et al., 2019). Recently, electrochromic smart window that can also store energy is becoming an attractive topic. Electrochromic smart window is based on the electrochromism to change the materials' optical properties under a small electric potential (Rauh, 1999). Generally, electrochromic materials with large transmittance modulation for vis- and near-IR light are preferred (Kim et al., 2015a; Yang et al., 2012). Similar to batteries or capacitors, electric energy can also be stored or released by charging or discharging the electrochromic materials. The energy can be stored through pseudocapacitance, i.e., the reversible faradic reactions at vicinities of electrodes (Conway et al., 1997; Fleischmann et al., 2020; Wang et al., 2012). Coloration efficiency (CE) is one of the most important parameters to evaluate the electrochromic smart windows. CE is defined as the optical density change (ΔOD) enabled by per unit charge (ΔQ) transmitting into or extracted from the electrochromic smart windows (Conway et al., 1997; Fleischmann et al., 2020; Wang et al., 2012). Traditionally, lower charge density materials are preferred for higher CE. However, for energy-storage smart windows, large charge density materials should be selected given their large energy storage capacity (Cao et al., 2019). In the following, some representative works about energy-storage electrochromic smart windows will be discussed from the aspects of fabrication methods, mechanisms, performances, and potential advantages.

WO_x is one of the mainstream electrochromic materials that exhibit excellent electrochromic performances (Arakaki et al., 1995; Yu et al., 2019). Yang et al. (2014) utilized WO_3 for fabricating large-scale electrochromic smart windows. Firstly, the WO_3 film was composed by growing WO_3 nanosized thin layer on FTO glasses with physical vapor deposition method. A high current (100 A) was applied on the raw material WO_3 powder, and a low pressure (4×10^{-4} Pa) was maintained for the reaction chamber. Then two electrodes were sealed into a cell with H_2SO_4 electrolyte. Figure 3.1a shows the SEM image of the synthesized WO_3 on the FTO glass. Figure 3.1b demonstrates the thin thickness from the cross-section view. Figure 3.1c is the AFM image of the film. Figure 3.1d shows the color change with the applied voltage. It was found that the transmittance change could be 63.7% for 633 nm incident light. However, Cao et al. (2019) found that WO_x exhibits low charge density and poor energy storage performance. By using Ta-doped TiO_2 nanocrystals, they fabricated a new smart window with charge storage density of at least two times higher than WO_x. During fabrication, the colloidal Ta-doped TiO_2 nanocrystals were composed with a one-pot method. Figure 3.1e shows the TEM image of the as-synthesized Ta-doped TiO_2 nanocrystals. Then the working electrode was prepared. The TiO_2 hexane solution was spin-coated on an ITO glass, followed by annealing at

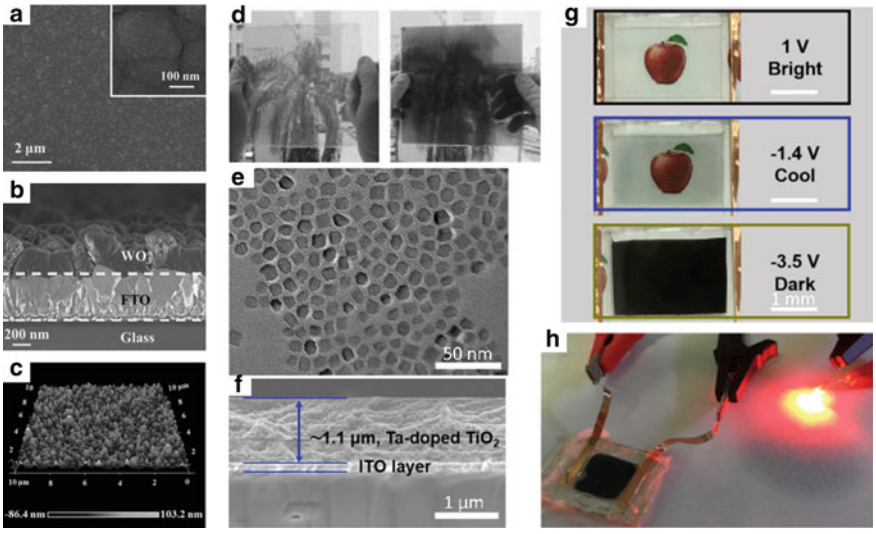

Fig. 3.1 The SEM images of **a** the synthesized WO_3 film (inset: the magnified SEM image) and **b** the cross-section of the layers of the film. **c** The AFM image of the WO_3 thin film. **d** The outdoor demonstration of the electrochromic behavior of the smart window. Reproduced with permission (Yang et al., 2014). Copyright by Wiley-VCH. **e** The TEM images of the as-prepared Ta-doped TiO_2 nanoparticles. **f** The SEM image of the cross-section of the Ta-doped TiO_2 film. **g** The digital images of the smart window at different voltages. **h** The smart window is powering a red LED. Reproduced with permission (Cao et al., 2019). Copyright by Cell Press

400 °C. Figure 3.1f shows the cross-section of the working electrode. Next, the NiO-based counter electrode was made by spin-coating a precursor solution containing $Ni(CH_3COO)_2{\cdot}4H_2O$, CH_3COOLi, and $Ti(OC_3H_7)_4$ in ethanol on an ITO glass, followed by annealing at 350 °C. Last, the working electrode and counter electrode were integrated into a cell with 0.5 mm spacing, and the electrolyte $LiClO_4$ was injected inside. This smart window can gradually change the color from transparent to dark under different voltages (see Fig. 3.1g, h). The outstanding energy storage of this smart window is demonstrated by easily lighting up a LED device.

Apart from the high performances, the fabrication technologies of smart windows are also important. Cai et al. (2017) fabricated large-area multifunctional smart windows using the inkjet printing method. Such a method has several advantages such as low cost, high-efficiency materials usage, and suitability for large-scale manufacturing (Corzo et al., 2019; Sundriyal & Bhattacharya, 2018; Xu et al., 2015). In their work, two CeO_2/TiO_2 and WO_3/PEDOT:PSS [poly(3,4-ethylenedioxythiophene)–poly(styrene sulfonate)] inks were developed. Both inks used the mixture of DI water, ethylene glycol, and diethylene glycol n-butyl ether as the solvent. Then the inks were printed on FTO-coated glasses, and dried at 60 °C for 2 h. The CeO_2/TiO_2 film needed additional 450 °C annealing for better adhesion. Finally, the smart window was fabricated by assembling the two films into cells with 2 mm spacing using H_2SO_4 as the electrolyte. Figure 3.2a–b show the SEM images of the printed CeO_2/TiO_2

and WO_3/PEDOT:PSS films. Figure 3.2c–d are the TEM images of the nanoparticles of the CeO_2/TiO_2 and WO_3/PEDOT:PSS. The reversible redox reactions on the electrodes are:

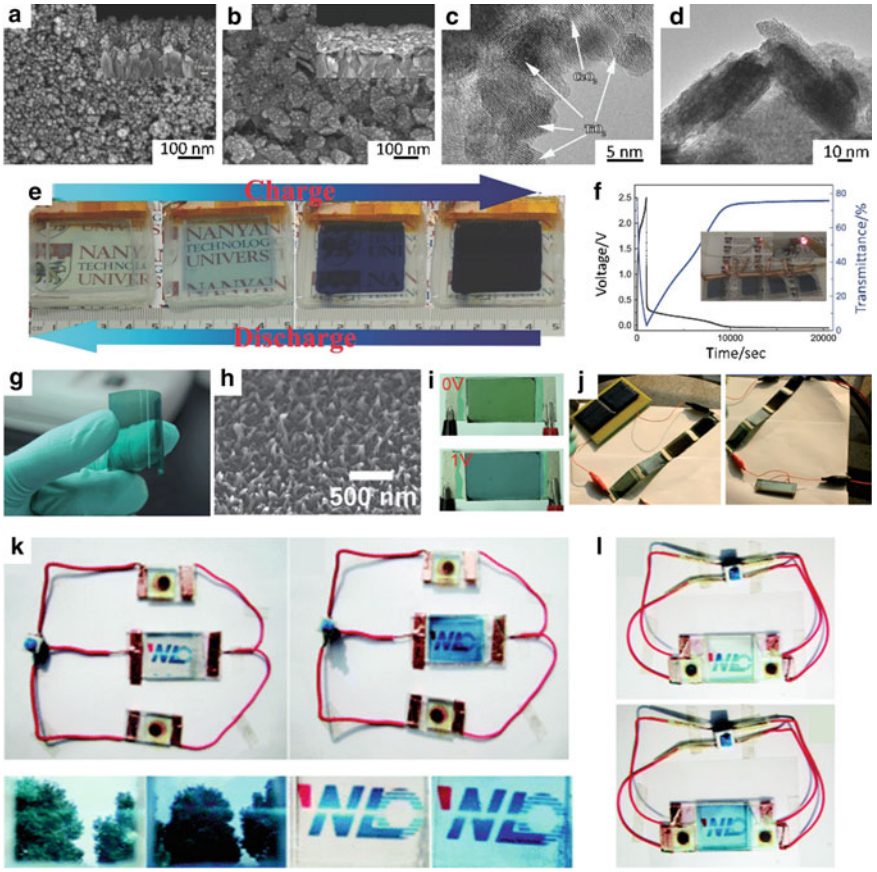

Fig. 3.2 The SEM images of printed **a** CeO_2/TiO_2 film and **b** WO_3/PEDOT:PSS film (insets: the magnified images). The TEM images of prepared **c** CeO_2/TiO_2 nanoparticles and WO_3/PEDOT:PSS nanoparticles. **e** The color change of the charging and discharging processes of the smart window. **f** The normal galvanostatic charging and slow discharging of the smart window and the corresponding optical responses (inset: a red LED can be lighted up with four devices connected in series). Reproduced with permission (Cai et al., 2017). Copyright by Wiley-VCH. **g** The digital image of a single electrode. **h** The morphology of the PANI nanowire array. **i** The images of the smart window at different voltages. **j** The smart windows are charging with a solar cell (left) and powering an LCD (right). Reproduced with permission (Wang et al., 2012). Copyright by Royal Society of Chemistry. The colored and bleached states of the Type I **k** and Type II **l** smart windows. Reproduced with permission (Xie et al., 2014). Copyright by Royal Society of Chemistry

$$WO_3 + xH^+ + xe^- \leftrightarrow H_xWO_3$$

$$PEDOT^+ \cdot PSS^- + H^+ + e^- \leftrightarrow PEDOT^0 \cdot PSS^- \cdot H^+$$

$$4CeO_2 + 4H^+ + 4e^- \leftrightarrow 2Ce_2O_3 + 2H_2O$$

$$TiO_2 + xH^+ + xe^- \leftrightarrow TiOOH$$

When the WO_3 and $PEDOT^+ \cdot PSS^-$ were reduced and Ce_2O_3 and TiOOH were oxidized, the materials would change the color from transparent into blue. Simultaneously, electric energy could be stored. Figure 3.2e demonstrates the color transition of the smart window during charging and discharging processes. The color of the device becomes darker from almost colorless with the applied electric potential. Figure 3.2f further displays the optical transmittance change for 633 nm incidental light. Notably, four devices connected in series can light up a commercial LED for two hours, demonstrating the efficiency of this inkjet printing method.

Apart from the optical performance and fabrication, excellent structural flexibility is also desired to adapt to different working environments. Using organic PANI (polyaniline) as the conductive material, Wang et al. (2012) developed a new flexible energy-storage smart window. In fabrication, a PEDOT:PSS in DMSO (dimethyl sulfoxide) solution was spin-coated on a PET film. Then PANI nanowire arrays were deposited on the film with a dilute polymerization process. Figure 3.2g shows a flexible electrode fabricated with PANI. Figure 3.2h shows the PANI nanowire arrays. Subsequently, two synthesized films were used as the electrodes with H_2SO_4-PVA gel electrolyte layer scrape-coated. Finally, the silver glue was applied to form the conducting paths and the cell was sealed. Figure 3.2i displays that the color of the smart window changed from light yellow at 0 V to deep blue with 1 V voltage. Notably, both the working and counter electrodes were the PANI-based. Thus, when a voltage is applied, only the PANI on the working electrode can change color. Large flexibility could be achieved by sacrificing certain transmittance modulations. Figure 3.2j demonstrates that commercial Si-based solar cells could be used to charge the smart window. Similarly, Xie et al. (2014) also integrated solar cells to power smart windows with self-fabricated dye-sensitized solar cell. The WO_3 electrochromic film was fabricated by electrochemically depositing on ITO glass with tungstic acid. Pt was deposited on ITO glasses as counter electrode. Then the smart window cells were fabricated by stacking and sealing the two electrodes with H_2SO_4-PVA gel as electrolyte. For solar cells, the TiO_2 electrode was manufactured by screen printing with commercial P25 TiO_2. After annealing at 500 °C and sensitized with ethanol solution, the TiO_2 electrode was integrated with Pt electrode into dye-sensitized solar cell using DMPII, LiI, I_2 and 4-TBP in methoxy propionitrile as electrolyte. Figure 3.2k–l show two designing strategies. For Type I (Fig. 3.2k), the

smart window was controlled by a single-pole-double-throw switch to selectively change between coloration and bleaching states. For Type II (Fig. 3.2l), the colorless and blue states can be reversibly changed under strong sunlight with a double-pole double-throw switch.

In addition to the electrochromic effect, new materials other than electrochromic materials can also be used for energy-storage smart windows. For example, Zhou et al. (2020) proposed a hydrogel-based smart window. The used hydrogel is a poly (N-isopropylacrylamide) (PNIPAm)-based network, which could reversibly change the transmittance at different temperatures. The mechanism was believed to be a hydrophilic to hydrophobic transition at lower critical solution temperature (LCST). The hydrogel can become transparent (high solar transmission) when the environmental temperature is lower than LCST and vice versa (Matsumoto et al., 2018; Wu et al., 2020). Moreover, the hydrogel can contain a large amount of water inside, showing outstanding thermal energy storage (~250 kJ kg^{-1}) and large specific heat capacity (4.2 kJ kg^{-1} K^{-1}). The hydrogel-based smart window can be manufactured by two steps. First, the hydrogel was synthesized with mixing NIPAm (N-isopropylacrylamide) monomer, the crosslinker acrylamide, the catalyst TEMED (N,N,N,N-tetramethylethylenediamine), and the initiator APS (ammonium peroxydisulfate). Second, the device can be assembled by pouring the hydrogel and DI water into a glass box and sealing. Figure 3.3 shows the samples at the meter scale. The window was transparent at lower temperatures and gradually changed into opaque at higher temperatures. Notably, this hydrogel-based smart window directly stored and released thermal energy instead of electric energy, which makes it tunable only by environmental temperature rather than electricity.

To conclude, smart windows can modulate indoor temperature by turning transmittance with the electrochromic effect. Specific materials such as WO_x and PANI could be used under different requirements. In addition to the color change under applied voltages, energy can also be stored on the electrodes through the electrochemical reactions, which enables more energy saving. Apart from the electrochromic

Fig. 3.3 The transmittance changes at different time of a day. The window is half filled with the hydrogel-based smart window. Reproduced with permission. (Zhou et al., 2020) Copyright by Cell Press

smart windows, other smart windows, such as hydrogel-based ones, also provide more choices. Instead of storing electricity, thermal energy from the environment is stored. This may provide some important insights since they do not need extra electricity input.

3.2.2 Combined Energy Saving and Self-powering

The electrochromic smart window is a good choice for energy-efficient buildings given its tunable transmittance by optical modulation and energy-storage capability. However, they usually need external power for charging and cannot intrinsically generate electricity. Here, in this section, we will discuss the strategies to construct self-powered smart windows.

The first method is by integrating a galvanic cell with the smart window. Wang et al. (2014) designed a self-rechargeable electrochromic smart window by integrating with aluminum electrodes. The electrochromic iron-based compound materials can be charged when the aluminum is oxidized. The benefit for the iron-based compound is that iron (II, III) hexacyanoferrate (II, III) (Prussian blue, PB) can be reduced to colorless Prussian white (PW), and the Prussian white can spontaneously oxidized with dissolved oxygen. The reactions are denoted as:

$$Al \leftrightarrow Al^{3+} + 3e^{-}$$

$$\mathrm{KFe}^{III}\left[\mathrm{Fe}^{II}(\mathrm{CN})_6\right](\mathrm{PB}) + \mathrm{K}^{+} + e^{-} \leftrightarrow \mathrm{K_2Fe}^{II}\left[\mathrm{Fe}^{II}(\mathrm{CN})_6\right](\mathrm{PW})$$

During fabrication, the PB films were first prepared by the electrochemical deposition method. Specifically, ITO glasses were coated in the mixture of K_3FeCN_6, $FeCl_3$, and KCl with current density 50 mA/cm^2. Then the cell was assembled by sealing the PB film and an ITO glass with an aluminum strip on one edge together and KCl as the electrolyte. Figure 3.4a demonstrates that the smart window can change the color with self-powering battery-like capabilities, as demonstrated by the LED lighting-up in Fig. 3.4a (i and ii) when two electrodes were connected at colored state. After changing into bleached state, the LED cannot be lighted (Fig. 3.4a, iii and iv). The cell can go back to the colored state when the electrodes were disconnected. Then the LED can be lighted again if the electrodes were connected at the colored state (Fig. 3.4a, v and vi). About 38.5% transmittance change could be achieved by this self-powered smart window.

Moreover, thermochromic smart window can tune optical transmittance by modulating the incident sunlight. Zhou et al. (2013) use the common VO_2 material (Cui et al., 2018, Chen et al., 2011, Li et al., 2017; Chen et al. 2019; Madida et al., 2014) and designed a thermochromic smart window that can generate electricity. The mechanism for the VO_2 thermochromic effect is attributed to the reversible metal-semiconductor phase transition (Chen et al., 2011; Cui et al., 2018; Golubev

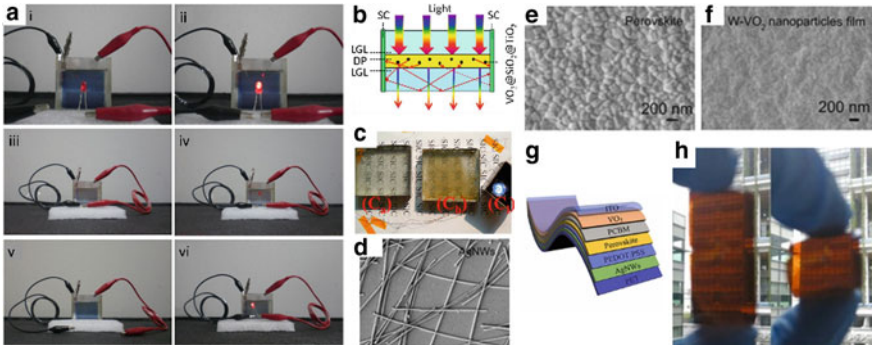

Fig. 3.4 **a** The performances of the smart window. (i) The two electrodes are disconnected at colored state. (ii) An LED is lighted up with electrodes connected. (iii) The bleached states with two electrodes connected. (iv) The LED is not powered with electrodes connected at bleached state. (v) The smart window is recovered with electrodes disconnected. (vi) The LED is lighted up. Reproduced with permission (Wang et al., 2014). Copyright by Nature Publishing Group. **b** The design strategy of the smart window. SC, LGL and DP denote the solar cell, light guider layer and low reflective index medium, respectively. **c** The smart window can power a 1.5 V LED. Reproduced with permission (Zhou et al., 2013). Copyright by Nature Publishing Group. The SEM images of **d** the AgNW arrays, **e** the perovskite film, and **f** the VO_2 film. **g** The schematic of the layers of the smart window. **h** The digital images of the perovskite/W-VO_2 film with different bending curvatures. Reproduced with permission (Meng et al., 2022). Copyright by Elsevier

et al., 2001). At a lower temperature, the VO_2 has a monoclinic crystalline structure and is transparent to the near-infrared light. At higher temperatures, the VO_2 turns into metallic state with a tetragonal crystal structure and reflects the near-infrared light (Miller & Wang, 2015; Wang et al., 2016a, 2018). The transition temperature is 68 °C (Hong-Chen et al., 2005; Wang et al., 2005, 2017). Therefore, the VO_2-based smart windows can automatically tune the indoor temperature by blocking/passing the incident light. To better use the scatted light, Zhou et al. (Zhou et al., 2013) assembled solar cells on both sides of the smart windows (Fig. 3.4b). The smart window consisted of light guider layers (LGL), low reflective index medium (DP), and solar cells on both sides. Thus, scattered lights can be picked by the solar cells without affecting the transmittance. To achieve better scattering effects and lower absorption by VO_2, a core-shell-shell $VO_2/SiO_2/TiO_2$ was synthesized. First, the core was synthesized by annealing V_2O_5 and oxalic acid at 240 °C. Then, the VO_2/SiO_2 was prepared with TEOS hydrolysis method. Third, the as-synthesized VO_2/SiO_2 were dispersed in ethanol, followed by adding tetrabutyl titanate and $NH_3(H_2O)$ for forming the $VO_2/SiO_2/TiO_2$. Next, the $VO_2/SiO_2/TiO_2$/PU composite film was prepared by mixing the particles, saline coupler KH-570 and polyurethane in DI water, and then casted on a PC plate. Finally, the smart window was assembled with the strategy shown in Fig. 3.4b. Thus, solar light could be scattered by this smart window and LED was lighted up at the same time (Fig. 3.4c).

In addition to embodying smart windows with energy-saving or energy-generating function, other solar devices can also be integrated for smart window functions. Meng

et al. (2022) integrated a perovskite solar cell that can both generate electricity and tune transmittance. Perovskite solar cell is a newly emerging solar cell with a high power conversion efficiency (Ansari et al., 2018; Chen et al., 2018; Li et al., 2018; Mei et al., 2014; Yin et al., 2014; Zhang et al., 2021). In this work, Meng et al. introduced a layer of Tungsten-doped VO_2 (W-VO_2) nanoparticles for thermochromic effect. The perovskite photovoltaic materials used was $Cs_{0.05}FA_{0.85}MA_{0.10}Pb\ (I_{0.97}Br_{0.03})_3$ and the electron transport layer was [6,6]-Phenyl-C_{60}-butyric acid methyl ester (PCBM) for better energy-level matching. The device was fabricated mainly by spin-coating method. First, a silver nanowire (AgNW) network was deposited on a PET film. The SEM image is shown in Fig. 3.4d. Then a layer of PEDOT:PSS was spin-coated onto the AgNW. Subsequently, a perovskite solution was spin-coated on the film with N_2 protection. The perovskite solution was synthesized by mixing CsI, MABr, PbI_2, FAI, and MACl in DMF/DMSO solution. The SEM image of the perovskite layer is shown in Fig. 3.4e. After annealing at 100 °C, the PCBM chlorobenzene solution was spin-coated, and then annealed at 90 °C. Next, BCP saturated solution was spin-coated. The last spin-coated layer was a Si-Al gel containing W-VO_2 and ethanol. Figure 3.4f displays the morphology of the W-VO_2 layer. After all the spin-coated layers were finished, a nanosized ITO layer was deposited on the film with magnetron sputtering method. The overall stacking strategy was illustrated in Fig. 3.4g. Its power conversion efficiency is about 16.1%. Since the window was fabricated with PET substrates, it also exhibits certain flexibility. Figure 3.4h shows the fabricated perovskite/VO_2 film at different bending curvature. The solar cell performance did not compromise much at a bending radius of 5 mm. Nonetheless, the transmittance of this window was not high, showing an average about 25.5% visible transmittance.

With the higher energy-saving requirements for green buildings, it is beneficial to design smart windows that are capable of both saving energy and self-powering or outputting power to other appliances. It is ideal if the unwanted incident sunshine can be utilized to generate electricity. Although the performances of this smart windows are not perfect due to the comprised transmittance when integrated with solar cells, these issues could be solved by future advancements of materials and fabrication technologies.

3.2.3 Combined Energy Saving and Self-cleaning

In addition to the above functionalities of storing and generating energy, smart windows can also be designed with reversible light transmittance and tunable wetting properties. Smart windows with tunable optical properties play a significant role in buildings given their potentials in modulating solar irradiation to tune buildings internal thermal conditions (Granqvist, 2016, Llordés et al., 2013; Cai et al., 2016; Cui et al., 2018; Ke et al., 2018; Khandelwal et al., 2017). Moreover, smart windows with tunable surface wettability that can achieve self-cleaning capability can provide many other applications, such as for architectural/vehicle windows with

better vision, microfluidic devices, and lab equipment surficial pollutant removement. In this section, multifunctional smart windows with switchable light transmittance and wetting tunability are discussed.

To date, reversible optical switching has been accomplished either by molecular arrangements change (Cupelli et al., 2009; Guo et al., 2017; Kim et al., 2015b), suspend particles (Vergaz et al., 2008), or by the oxidation-reduction reaction of chromogenic materials (Granqvist, 2014, 2000; Bechinger et al., 1996) stimulated by external light (Wu et al., 2017), or electrical (Dyer et al., 2007; Gesheva et al., 2012), thermal (Zheng et al., 2015), and chemical (Zhang et al., 2017a) factors. However, these smart windows are either chemically unstable during optical switch or difficult to prepare (Lampert, 2004). Thus, a rather simple and high efficient method based on mechanical wrinkling is proposed to fabricate multifunctional smart windows with integrated fast transparency switch and tunable surficial wettability. Surface wrinkling for smart window relies on the dynamical and reversible surface morphology manipulation. Bowden et al. (1998) first reported the fabrication of gold nanoscale surface patterning through wrinkling of gold nanofilms on soft poly (dimethylsiloxane) (PDMS) substrate. After coated on PDMS substrate at an elevated temperature, the gold nanofilm could be compressed due to the larger thermal expansion coefficient in PDMS substrates during cooling. When temperature goes beyond a critical value, spontaneous ordered and disordered wrinkling surface patterns occur at small scales. Thereafter, surface wrinkling with both flat surface and multileveled micro-structures have been extensively studied for dynamic scaffolds (Kim et al., 2010), tunable diffraction gratings (Harrison et al., 2004), microlens arrays (Chan & Crosby, 2006), and flexible electronic devices (Chandra et al., 2007), as well as multifunctional smart windows with transparency/wettability tunability (Jiang et al., 2018; Ke et al., 2019a; Khang et al., 2006; Kim et al., 2013, 2018; Lee et al., 2010; Li et al., 2021b; Lin et al., 2018; Tomholt et al., 2020; Zhang et al., 2017b).

The wrinkled surface morphology characterized by the wrinkle periodicity and height is mainly determined by the applied mechanical strain. Thus, it exhibits high controllability and dynamical tunability, making it promising for constructing mechanochromic (MC) smart windows. Here, we discuss several representative MC smart windows with different patterned (micro/nano-pillar (Lee et al., 2010), anisotropy (Kim et al., 2013), self-similar (Lin et al., 2018), additional delamination buckling (Zhang et al., 2017b) and cracks-based (Tomholt et al., 2020) surface morphologies.

Figure 3.5a (i) illustrates the procedures to pattern structured PDMS films with surface wrinkles. AAO (anodic aluminum oxide) templates with nanopore were first fabricated by a two-step anodization. The template surface was then treated with octadecyltrichlorosilane for easy releasing and preparation of multiple replicated PDMS structures. Uncured PDMS was poured over the patterned AAO template and cured. The PDMS film was then peeled off from the template. Next, the nanopillar structured PDMS film was uniaxially stretched and exposed to ultraviolet-ozone (UVO) radiation. (Heptadecafl uoro-1,1,2,2-tetrahydrodecyl) trichlorosilane is coated on the stretched PDMS film to achieve the enhanced tunable wettability. Finally, periodic wavy microstructures were generated on the PDMS substrate upon

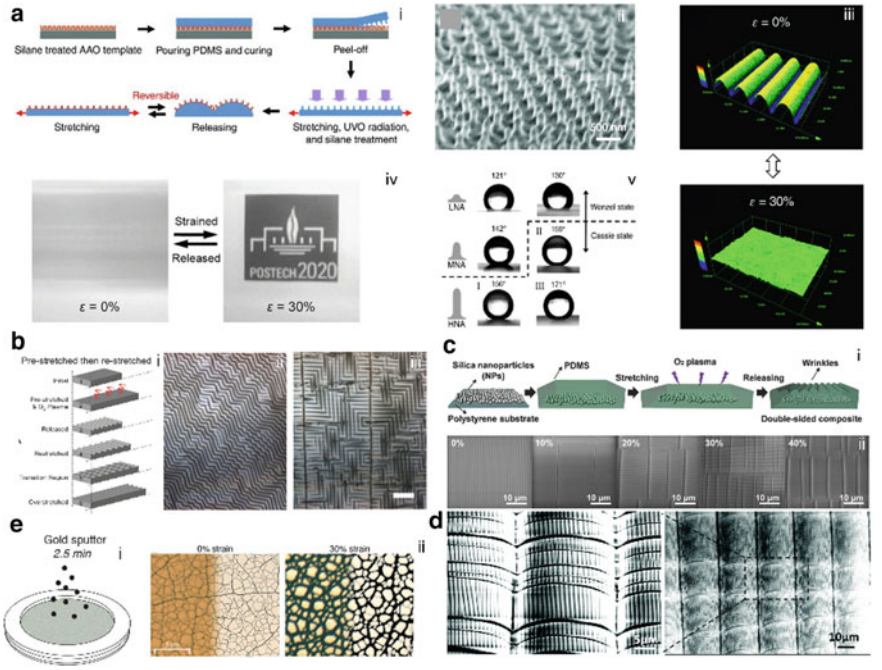

Fig. 3.5 Different fabrication strategies of MC smart windows. **a**–**d**, wrinkle based with nanopillar microstructure **a** (Lee et al., 2010), surficial anisotropy **b** (Kim et al., 2013), multiple states **c** (Kim et al., 2018) and self-similarity **d** (Lin et al., 2018). **e**, MC smart window with cracks (Tomholt et al., 2020). Reproduced with permissions. Copyright by Wiley Publishing Group

releasing the pre-stretched strain with preserved nanopillars. The nanopillar patterned wrinkling could be reversibly flattened upon stretching, but the nanopillar pattern remained. Figure 3.5a (ii) shows the SEM image on the features of the micro-wrinkling surface with nanopillars. It forms a very well-ordered and uniform microscopic pillar structures (with height ~300 nm and diameter ~150 nm) with hexagonal non-close-packed arrays on the micro-wrinkles (with 31 μm wavelength and 4.4 μm amplitude) over a large area without collapse. The confocal laser scanning microscopy (CLSM) images (Fig. 3.5a (iii)) demonstrated that the micro-wrinkle pattern morphs under the applied uniaxial mechanical strain. Gradually increasing the applied strain decreases the wrinkle amplitude and finally leaves only the nanopillar structures

Figure 3.5a (iv) shows that reversible opaque to transparent transition upon re-stretching the wrinkled sample, where the optical transmittance increases from 9.2 at 0% applied strain to 92 at 30% strain. The opacity is arising from the extensive scattering of light induced by the periodic micrometer-sized wrinkling surface. The tapered periodic nanopillar arrays produced the gradient effective refractive index that increases from the pillar peaks to the pillar troughs bypassing the pillar bodies. Thus, the entire visible spectrum is minimally reflected. For wettability of

this wrinkle structured surface, the contact angle increases when the surface structure becomes rougher (i.e., micro-wrinkle appears or the aspect ratio of nanopillar increases). For strained or released films, the contact angle hysteresis increases with the surface roughness. Water droplets can easily penetrate the valleys between the low-aspect-ratio nanopillars with similar height. Then, a continuous stable solid-liquid-gas (three-phase) contact line would be created with high water adhesion, thus, water droplet could become pinned firmly on the surface without any sliding even though the samples were vertically titled. However, for either strained or released nanopillar arrays with relatively higher aspect ratios, the surface exhibits superhydrophobicity with water contact angle larger than 150° and contact angle hysteresis less than 10°. Water droplet on this surface was in Cassie state and can easily roll away.

In addition to uniaxial mechanical strain, sequential stretching methods have also been studied to generate multiple state and self-similar wrinkling microstructures. Figure 3.5b (Kim et al., 2013) shows that upon stretching the wrinkled PDMS film, three different types of wrinkling morphologies can be generated with changing wavy direction. Moreover, treating soft PDMS substrates with embedded stiff silica nanoparticles (Fig. 3.5c (i); Chandra et al., 2007), the modulus mismatch enables multiple micro-structured wrinkled surfaces, where the micro-wrinkles can change from a uniform to nonuniform form with studs upon increasing the stretching strain. Similarly, by following the two-stage stretching-releasing procedure, micro-wrinkled structures with self-similarity (Lin et al., 2018) could be achieved, which exhibits multistate optical transmittance (from totally bluish to intermediate state with structural color and finally transparency by increasing the stretching strain) and controllable droplet transport behaviors (pinning to rolling away). High strain sensitivity of transmittance with low mechanical strain and crack-free micro-wrinkle pattern can be achieved by applying biaxial mechanical strains (Ke et al., 2019a).

When the bonding between soft substrate and top stiff layer (for example embedded with metal/crystalline nanoparticles) is weak, buckling driven delamination or cracks in the stiff top layer can occur. Buckling delamination forms from the local blisters to larger periodic patterns with the increasing compression strain. Compared to wrinkling, buckling delamination can tolerate relatively large strains (Thomas et al., 2015; Zang et al., 2013, 2017b; Zhang & Yin, 2018), which makes it promising for smart windows with extreme tunable optical properties. Combined wrinkle-crack surface microstructures could enhance surface roughness and thus strengthen the optical scattering effect (Zeng et al., 2016). Figure 3.5d shows that wrinkled PDMS coated with gold-based nanoparticles could generate cracks after air inflation, resulting from the nonuniform strain field along the radial direction. After deflation, cracks would disappear. Thus, the coated gold layer can tune the near-infrared transmission to change the indoor thermal environment, while the combined wrinkles and cracks can tune the visual effect (Tomholt et al., 2020).

To date, most MC smart windows are developed by surface instability while more advancing methods are emerged with promising performances (Ke et al., 2019a). However, for practical commercialized applications, challenges still exist and need to be addressed. For example, the mechanical strains need to be smaller to generate a

large transmittance modulation and the mechanical robustness of such smart windows need to be improved for long-time endurance.

3.2.4 Combined Energy Saving and Water Harvesting

Harvesting water from air is promising for solving the water crisis all around the world (Zhai et al., 2006; Fathieh et al. 2018; Lekouch et al., 2011). Water harvesting includes water/fog condensation, droplet transport and collection. The large-area windows in modern buildings become an ideal platform to not only save energy but also harvest and collect water from the environment. The tunable surface wettability of smart windows can control the water droplets' transport for collection and water harvesting functionality. In the following, different smart windows with water droplet movement control are discussed based on several representative works.

Achieving effective repulsion of low-surface-tension liquids on solid substrate is necessary for fine droplets control. Creating liquid-infused surface on porous film-based substrates provides an efficient method. Figure 3.6a illustrates the process to fabricate the temperature-responsive liquid infused porous surfaces (Zhai et al., 2006) for controlling water droplet movement at room temperature. The underlying mechanism is based on the paraffin that can easily change from a solid to liquid state upon temperature changes. Water droplets on this composite surface would be repelled or pinned responding to the environmental temperature. The left figure in Fig. 3.6a shows that the porous surfaces are composed of chitin nanofibers and poly(acrylic acid) and formed through the layer-by-layer self-assembly (see the SEM images in Fig. 3.6a, right), followed by introducing the mixed solidifiable and liquid paraffin into the hydrophobic nanofibrous surfaces as lubricant oil layer. Consequentially, the solidification of the paraffin changes the surface morphology and the solidifiable/liquid paraffin mixing control the droplets' movement. Figure 3.6a (right-bottom) shows that the contact angle of the droplets sharply decreased with the increasing temperature. For example, for a 1: 25 solidifiable/liquid paraffin surface, the droplet's contact angle can decrease rapidly from near 99–53° when increasing the temperature from 22 °C to the paraffin melting point near 28 °C. The sliding angle of the water droplet would decrease with the temperature and switched from an immobilized state to free sliding. This is attributed to the change of surface tension that improves the droplet mobility. At a low temperature (<22 °C), water droplets would be pinned even when the paraffin surface was titled to 90°. At a high temperature, water droplets will be cloaked by the lubricant fluid that is easy to evaporate, thus, the contact angle will increase to propel the droplets and roll away. However, at a low temperature, water droplets will not be cloaked and become pinned by the stable paraffin layer.

Compared to the chemical treatment, mechanical strains are preferred to tune the micro-surface wettability given its simplicity. As demonstrated by Lin et al. (Lin et al., 2017), self-similar hierarchical wrinkles (Fig. 3.6b, left) have been verified to exhibit excellent droplet movement control behavior. As shown in Fig. 3.6b (right),

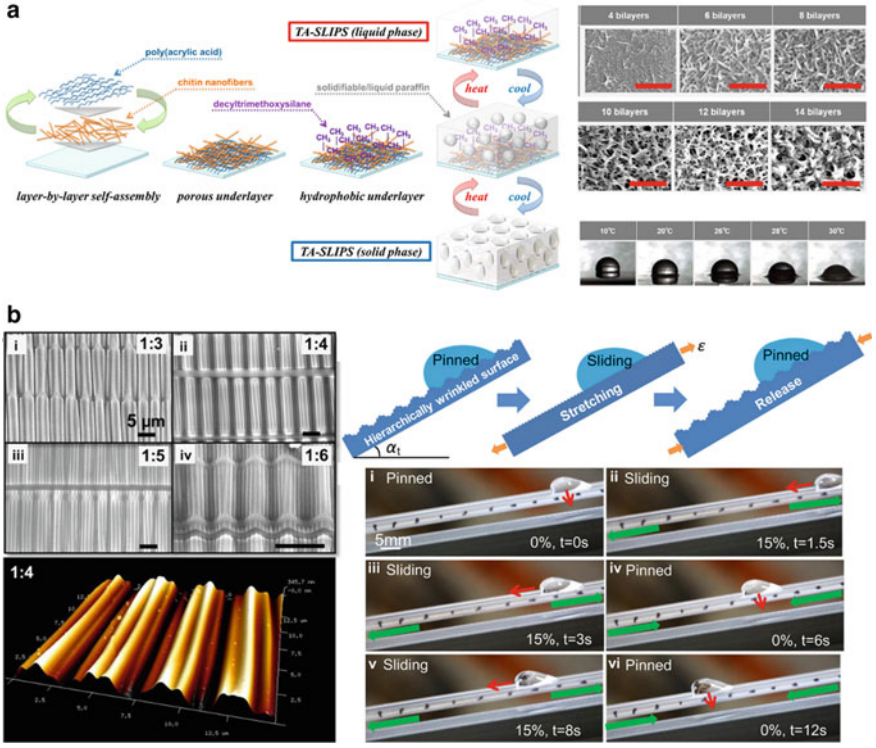

Fig. 3.6 Multifunctional smart windows for water droplet movement control. **a** Liquid-infused surface covered with paraffin. Reproduced with permission (Zhai et al., 2006). Copyright by Royal Society of Chemistry. **b** Self-similar hierarchical wrinkled smart window (Lin et al., 2017). Reproduced with permissions. Copyright by ACS Publications

the water droplets were initially pinned on the micro-wrinkled structure surface. After stretching, the pinned water droplet would slide. Due to the larger surface roughness, the droplet on the wrinkled surface would be in a Wenzel wetting state. When the wrinkled surface is stretched, its surface roughness decreases, which weakens the Wenzel effect and the water droplet loses its balance to slide.

Thus, by chemically or mechanically treating surface with different nano-/microstructures, smart windows could be effectively utilized to better collect water from the environmental air. However, water droplets are also highly dependent of the harvester's macroscopic geometry for high efficient delivery (Bai et al., 2020). Therefore, amounts of water harvesters with distinct geometrical forms have been proposed, such as cactus-like cone arrays (Ju et al., 2012; Lee et al., 2019) and gradient structural components (Xu et al., 2016). However, these water harvesters are challenging to be integrated with smart windows due to their unsuitable structural shapes. Recently, a highly stretchable kirigami structure has been proposed for multifunctional smart window applications that demonstrate efficient energy

saving by dynamically blocking (Tang et al., 2017; Yi et al., 2018), modulating (Ke et al., 2019b), energy-transforming (Lamoureux et al., 2015) solar light and as well collecting water (Bai et al., 2020; Li et al., 2021a).

For kirigami structures with parallel slits, uniaxial stretching can simply buckle sectional strips and generate periodic arrays of pores to tune the thermal condition inside buildings. Figure 3.7a shows that Tang et al. (2017), Yi et al. (2018) used the reflective kirigami structure with periodically distributed parallel cuts as an integrated system for designing environmental adaptive building envelopes. When constructing the kirigami structure with temperature-responsive shape memory polymers (Fig. 3.7a, top), the integrated kirigami design could actively open or close its pores in response to environmental temperature change. Both simulation and experimental results show that the generated arrays of pores and adaptively tilted ribbons could collectively diffuse the sunlight more evenly for electricity saving. Ke et al. (2019b) have recently proposed a bi-functional kirigami smart windows by embedding the elastomer with plasmonic vanadium dioxide (VO_2) nanoparticles (Fig. 3.7b, left). It has similar working mechanisms as the VO_2 based thermochromic smart windows discussed in Sect. 3.2.3. The structural geometry change can tune the visible light while the temperature-dependent localized surface plasmon resonance (LSPR) can tune the ultraviolet, visible and near-infrared light regions. With the increase of the temperature, the transmittance in the UV-vis-NIR can reduce from 75% (opened state) to nearly 0% (close state). This work opens a new avenue by integrating both macroscopic structure and composition materials to facilitate enhanced solar energy modulation. Moreover, attributing to the dynamically tunable tilted strips, researchers also designed kirigami-based smart windows that are capable of generating energy by mounting with photovoltaic materials to transform solar right into electricity (Fig. 3.7c, (Lamoureux et al., 2015)).

Additionally, after coating with hydrophobic treatments, kirigami structures can be designed with unique local geometries for water harvesting. Kirigami sheets in triangular cut patterns coated with hydrophobic infused paraffin materials could directionally and continuously collect water droplets from the environment. Recently, by introducing origami folds to kirigami sheet, Li et al. (2021a) invented an aerodynamics-assisted kirigami water harvester that can be scalable to the meter scale. Figure 3.8b (right) shows that stretching the kirigami sheet assisted with folds can transform the sheet into a 3D structure with periodically distributed pyramidal local pop-ups. Thus, the fluid-structure interactions lead to the formation of tube-like vortices penetrating through the opening pores. Near the cortex core, droplets would be attracted and accumulated, finally getting ejected to the collectors with their growing size. Based on the 1 m^2 (Fig. 3.8b, right-bottom) sample, this design was demonstrated with highly feasible and excellent collection rates up to 3.5 kg/h, which is 2.71 times from wire mesh structure. The water harvesting behavior of this design is mainly determined by the macroscopic structure rather than the coating materials as demonstrated in (Li et al., 2021a) after testing large amounts of different hydrophobic materials (Fig. 3.8b (left)). It should be noted that in addition to the kirigami structures, structure-based smart windows can also be extended to other forms such as origami and rigid mechanisms (Ke et al., 2019a; Li et al., 2021b).

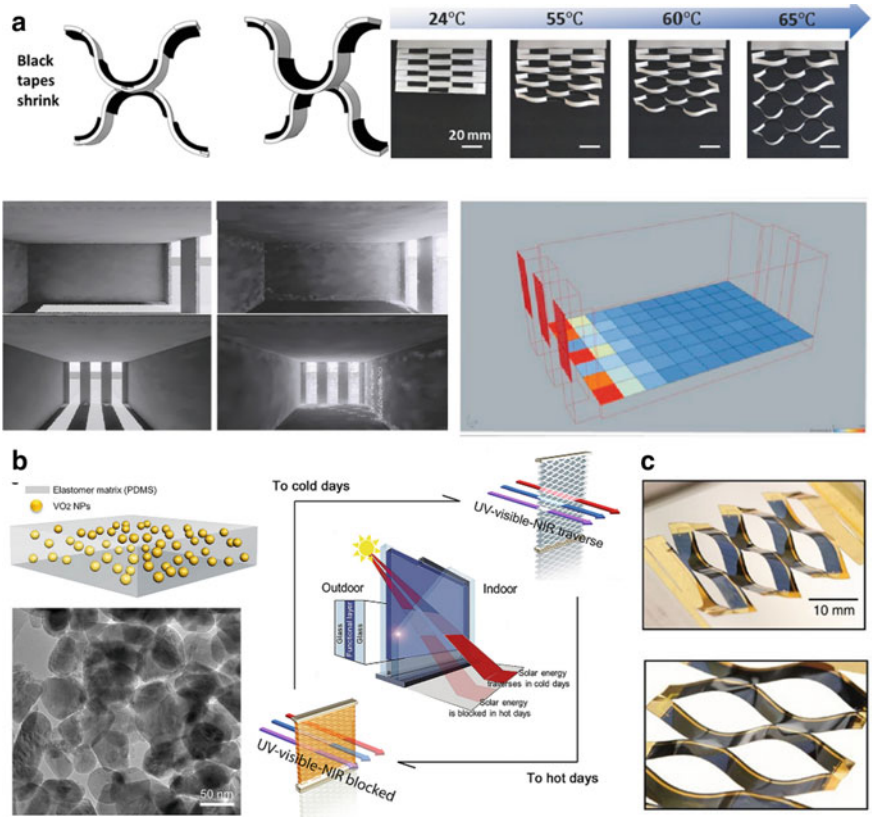

Fig. 3.7 Kirigami based smart window with dynamically tunable optical transmittance for energy saving and generation. **a** Thermally tunable kirigami façade with shape memory polymers (Tang et al., 2017; Yi et al., 2018). Reproduced with permissions. Copyright by Wiley Publishing Group and Elsevier. **b** Bifunctional kirigami based smart window fabricated by VO_2-embedded elastomers (Ke et al., 2019b). Reproduced with permission. Copyright by Cell Press. **c** Dynamic kirigami structure mounted with photovaltic material for energy generation (Lamoureux et al., 2015), Reproduced with permission. Copyright by Nature Publishing Group

3.3 Conclusion and Outlook

This chapter summarizes the advancement in smart windows with novel functionalities, such as energy storage, energy generation, self-cleaning, and water harvesting. We discussed several representative works from the perspectives of working mechanisms, materials synthesis, device fabrication, characterization, and functionality. Specifically, electricity can be stored by electrochemical reactions for the energy-storage electrochromic smart windows; some smart windows can utilize the scattered sunlight to generate electricity for self-powering during modulating the indoor light irrigation; by tuning the hydrophobicity, smart windows can self-clean by washing

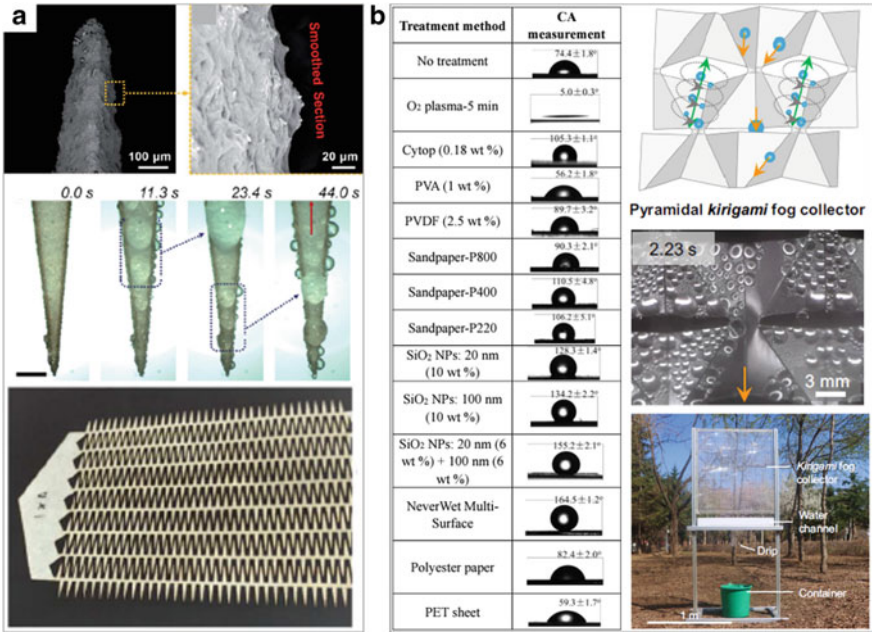

Fig. 3.8 Kirigami-based structures for water harvesting (Li et al., 2021a). Reproduced with permission. Copyright by Nature Publishing Group

away dusts to keep high performance; smart windows with special structures or by turning wettability can also harvest water, which is vital for energy and resource saving in drought areas.

Despite the advantages of the novel functionalities, limitations and challenges still remain for the current state-of-the-art smart windows. First, some smart windows do need energy input. For example, the electrochromic smart windows need charging, and the mechanochromic smart windows require mechanical loads for structure shifting. Second, the light transmittance modulations need improvements. For instance, some functionalities such as energy generation are achieved by sacrificing the light transmittance. The transmittance shifting temperature for VO_2 is about 68 °C, which is too high in terms of the practical use. Third, transmittance manipulation of some smart windows is fully passive.

Therefore, to overcome the issues, future studies are needed to improve the transmittance with lower or even zero energy consumption, harvesting energy from undesired sunlight without reducing the transmittance modulation, and better controllability by using high-performance materials and more novel designs. Furthermore, some new smart windows that harvest heat from the environment instead of sunlight, such as hydrogel-based smart windows, may also be a promising trend. Additionally, although adaptive façades have been developed for energy saving, such as the examples shown in Fig. 3.9, smart windows combined with adaptive façade are still little investigated. In terms of scalability, not only the performances of smart windows are

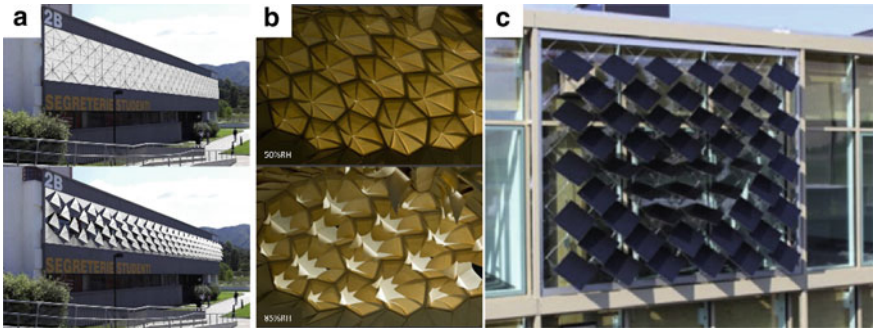

Fig. 3.9 **a** Fully-closed and open façades. Reproduced with permission (Cimmino et al., 2017) Copyright by Elsevier. **b** Adaptive façades actuated by moisture. Reproduced with permission (Reichert et al., 2015) Copyright by Elsevier. **c** The adaptive solar façades on the House of Natural Resources at ETH Zurich. Reproduced with permission (Powell et al., 2018) Copyright by Elsevier

needed to improve, but also simpler and more economic manufacturing methods are also preferred. Lastly, we hope this chapter can provide some insights for the future smart window designs for green building research and industry.

Acknowledgments The authors acknowledge the funding support from NSF (CMMI2005374) and NSF (CMMI-2013993), United States.

References

Aburas, M., Soebarto, V., Williamson, T., Liang, R., Ebendorff-Heidepriem, H., & Wu, Y. (2019). Thermochromic smart window technologies for building application: A review. *Applied Energy, 255*, 113522.

Ansari, M. I. H., Qurashi, A., & Nazeeruddin, M. K. (2018). Frontiers, opportunities, and challenges in perovskite solar cells: A critical review. *Journal of Photochemistry and Photobiology c: Photochemistry Reviews, 35*, 1–24.

Arakaki, J., Reyes, R., Horn, M., & Estrada, W. (1995). Electrochromism in NiOx and WOx obtained by spray pyrolysis. *Solar Energy Materials and Solar Cells, 37*, 33–41.

Azens, A., & Granqvist, C. (2003). Electrochromic smart windows: Energy efficiency and device aspects. *Journal of Solid State Electrochemistry, 7*, 64–68.

Baetens, R., Jelle, B. P., & Gustavsen, A. (2010). Properties, requirements and possibilities of smart windows for dynamic daylight and solar energy control in buildings: A state-of-the-art review. *Solar Energy Materials and Solar Cells, 94*, 87–105.

Bai, H., Zhao, T., Wang, X., Wu, Y., Li, K., Yu, C., Jiang, L., & Cao, M. (2020). Cactus kirigami for efficient fog harvesting: Simplifying a 3D cactus into 2D paper art. *Journal of Materials Chemistry A, 8*, 13452–13458.

Bechinger, C., Ferrere, S., Zaban, A., Sprague, J., & Gregg, B. A. (1996). Photoelectrochromic windows and displays. *Nature, 383*, 608–610.

Bowden, N., Brittain, S., Evans, A. G., Hutchinson, J. W., & Whitesides, G. M. (1998). Spontaneous formation of ordered structures in thin films of metals supported on an elastomeric polymer. *Nature, 393*, 146–149.

Cai, G., Darmawan, P., Cheng, X., & Lee, P. S. (2017). Inkjet printed large area multifunctional smart windows. *Advanced Energy Materials, 7*, 1602598.

Cai, G., Wang, J., & Lee, P. S. (2016). Next-generation multifunctional electrochromic devices. *Accounts of Chemical Research, 49*, 1469–1476.

Cao, S., Zhang, S., Zhang, T., Yao, Q., & Lee, J. Y. (2019). A visible light-near-infrared dual-band smart window with internal energy storage. *Joule, 3*, 1152–1162.

Casini, M. (2018). Active dynamic windows for buildings: A review. *Renewable Energy,* 119**,** 923–934.

Chan, E. P., & Crosby, A. J. (2006). Fabricating microlens arrays by surface wrinkling. *Advanced Materials, 18*, 3238–3242.

Chandra, D., Yang, S., & Lin, P.-C. (2007). Strain responsive concave and convex microlens arrays. *Applied Physics Letters, 91*, 251912.

Chen, C., Liu, D., Zhang, B., Bi, W., Li, H., Jin, J., Chen, X., Xu, L., Song, H., & Dai, Q. (2018). Carrier interfacial engineering by bismuth modification for efficient and thermoresistant perovskite solar cells. *Advanced Energy Materials, 8*, 1703659.

Chen, S., Wang, Z., Ren, H., Chen, Y., Yan, W., Wang, C., Li, B., Jiang, J., & Zou, C. (2019). Gate-controlled VO2 phase transition for high-performance smart windows. *Science Advances, 5*, eaav6815.

Chen, Z., Gao, Y., Kang, L., Du, J., Zhang, Z., Luo, H., Miao, H., & Tan, G. (2011). VO2-based double-layered films for smart windows: Optical design, all-solution preparation and improved properties. *Solar Energy Materials and Solar Cells, 95*, 2677–2684.

Chun, S. Y., Park, S., Lee, S. I., Nguyen, H. D., Lee, K.-K., Hong, S., Han, C.-H., Cho, M., Choi, H.-K., & Kwak, K. (2021). Operando Raman and UV-Vis spectroscopic investigation of the coloring and bleaching mechanism of self-powered photochromic devices for smart windows. *Nano Energy, 82*, 105721.

Cimmino, M. C., Miranda, R., Sicignano, E., Ferreira, A. J. M., Skelton, R. E., & Fraternali, F. (2017). Composite solar façades and wind generators with tensegrity architecture. *Composites Part b: Engineering, 115*, 275–281.

Conway, B. E., Birss, V., & Wojtowicz, J. (1997). The role and utilization of pseudocapacitance for energy storage by supercapacitors. *Journal of Power Sources, 66*, 1–14.

Corzo, D., Almasabi, K., Bihar, E., Macphee, S., Rosas-Villalva, D., Gasparini, N., Inal, S., & Baran, D. (2019). Digital inkjet printing of high-efficiency large-area nonfullerene organic solar cells. *Advanced Materials Technologies, 4*, 1900040.

Cui, Y., Ke, Y., Liu, C., Chen, Z., Wang, N., Zhang, L., Zhou, Y., Wang, S., Gao, Y., & Long, Y. (2018). Thermochromic VO2 for energy-efficient smart windows. *Joule, 2*, 1707–1746.

Cupelli, D., Pasquale Nicoletta, F., Manfredi, S., Vivacqua, M., Formoso, P., De FILPO, G., & Chidichimo, G. 2009. Self-adjusting smart windows based on polymer-dispersed liquid crystals. *Solar Energy Materials and Solar Cells, 93*, 2008–2012.

DOE. 2021. DOE Launches International Clean Energy Initiatives to Tackle Climate Crisis. In Energy, D. O. (Ed.). https://www.energy.gov/articles/doe-launches-international-clean-energy-initiatives-tackle-climate-crisis.

Dussault, J.-M., Gosselin, L., & Galstian, T. (2012). Integration of smart windows into building design for reduction of yearly overall energy consumption and peak loads. *Solar Energy, 86*, 3405–3416.

Dyer, A. L., Grenier, C. R. G., & Reynolds, J. R. (2007). A Poly(3,4-alkylenedioxythiophene) electrochromic variable optical attenuator with near-infrared reflectivity tuned independently of the visible region. *Advanced Functional Materials, 17*, 1480–1486.

EU. 2020. 2050 long-term strategy. In European Commission, E. U. (Ed.). https://ec.europa.eu/clima/eu-action/climate-strategies-targets/2050-long-term-strategy_en.

Fathieh, F., Kalmutzki Markus, J., Kapustin Eugene, A., Waller Peter, J., Yang, J., & Yaghi Omar, M. (2018). Practical water production from desert air. *Science Advances, 4*, eaat3198.

Fleischmann, S., Mitchell, J. B., Wang, R., Zhan, C., Jiang, D.-E., Presser, V., & Augustyn, V. (2020). Pseudocapacitance: From fundamental understanding to high power energy storage materials. *Chemical Reviews, 120*, 6738–6782.

Ge, D., Lee, E., Yang, L., Cho, Y., Li, M., Gianola, D. S., & Yang, S. (2015). A robust smart window: Reversibly switching from high transparency to angle-independent structural color display. *Advanced Materials, 27*, 2489–2495.

Gesheva, K. A., Ivanova, T. M., & Bodurov, G. (2012). Transition metal oxide films: Technology and "smart windows" electrochromic device performance. *Progress in Organic Coatings, 74*, 635–639.

Golubev, V. G., Davydov, V. Y., Kartenko, N. F., Kurdyukov, D. A., Medvedev, A. V., Pevtsov, A. B., Scherbakov, A. V., & Shadrin, E. B. (2001). Phase transition-governed opal–VO2 photonic crystal. *Applied Physics Letters, 79*, 2127–2129.

Granqvist, C. G. (2000). Electrochromic tungsten oxide films: Review of progress 1993–1998. *Solar Energy Materials and Solar Cells, 60*, 201–262.

Granqvist, C. G. (2014). Electrochromics for smart windows: Oxide-based thin films and devices. *Thin Solid Films, 564*, 1–38.

Granqvist, C. G. (2016). Recent progress in thermochromics and electrochromics: A brief survey. *Thin Solid Films, 614*, 90–96

Guo, S.-M., Liang, X., Zhang, C.-H., Chen, M., Shen, C., Zhang, L.-Y., Yuan, X., He, B.-F., & Yang, H. (2017). Preparation of a thermally light-transmittance-controllable film from a coexistent system of polymer-dispersed and polymer-stabilized liquid crystals. *ACS Applied Materials and Interfaces, 9*, 2942–2947.

Guterres, A. (2020). Carbon neutrality by 2050: the world's most urgent mission. In U. Nations (Ed.). https://www.un.org/sg/en/content/sg/articles/2020-12-11/carbon-neutrality-2050-the-world%E2%80%99s-most-urgent-mission.

Harrison, C., Stafford, C. M., Zhang, W., & Karim, A. (2004). Sinusoidal phase grating created by a tunably buckled surface. *Applied Physics Letters, 85*, 4016–4018.

Hong-Chen, W., Xin-Jian, Y., Jian-Jun, L., & Yi, L. (2005). Fabrication and characterization of nanocrystalline VO 2 thin films. *Chinese Physics Letters, 22*, 1746–1748.

Isaac, M., & van Vuuren, D. P. (2009). Modeling global residential sector energy demand for heating and air conditioning in the context of climate change. *Energy Policy, 37*, 507–521.

Jiang, B., Liu, L., Gao, Z., & Wang, W. (2018). A general and robust strategy for fabricating mechanoresponsive surface wrinkles with dynamic switchable transmittance. *Advanced Optical Materials, 6*, 1800195.

Ju, J., Bai, H., Zheng, Y., Zhao, T., Fang, R., & Jiang, L. (2012). A multi-structural and multi-functional integrated fog collection system in cactus. *Nature Communications, 3*, 1247.

Kamalisarvestani, M., Saidur, R., Mekhilef, S., & Javadi, F. S. (2013). Performance, materials and coating technologies of thermochromic thin films on smart windows. *Renewable and Sustainable Energy Reviews, 26*, 353–364.

Ke, Y., Chen, J., Lin, G., Wang, S., Zhou, Y., Yin, J., Lee, P. S., & Long, Y. (2019a). Smart windows: Electro-, thermo-, mechano-, photochromics, and beyond. *Advanced Energy Materials, 9*, 1902066.

Ke, Y., Yin, Y., Zhang, Q., Tan, Y., Hu, P., Wang, S., Tang, Y., Zhou, Y., Wen, X., Wu, S., White, T. J., Yin, J., Peng, J., Xiong, Q., Zhao, D., & Long, Y. (2019b). Adaptive thermochromic windows from active plasmonic elastomers. *Joule, 3*, 858–871.

Ke, Y., Zhou, C., Zhou, Y., Wang, S., Chan, S. H., & Long, Y. (2018). Emerging thermal-responsive materials and integrated techniques targeting the energy-efficient smart window application. *Advanced Functional Materials, 28*, 1800113.

Khandelwal, H., Schenning, A. P. H. J., & Debije, M. G. (2017). Infrared regulating smart window based on organic materials. *Advanced Energy Materials, 7*, 1602209.

Khang, D.-Y., Jiang, H., Huang, Y., & Rogers John, A. (2006). A stretchable form of single-crystal silicon for high-performance electronics on rubber substrates. *Science, 311*, 208–212.

Kim, H.-N., Ge, D., Lee, E., & Yang, S. (2018). Multistate and on-demand smart windows. *Advanced Materials, 30*, 1803847.

Kim, J., Ong, G. K., Wang, Y., Leblanc, G., Williams, T. E., Mattox, T. M., Helms, B. A., & Milliron, D. J. (2015a). Nanocomposite architecture for rapid, spectrally-selective electrochromic modulation of solar transmittance. *Nano Letters, 15*, 5574–5579.

Kim, J., Yoon, J., & Hayward, R. C. (2010). Dynamic display of biomolecular patterns through an elastic creasing instability of stimuli-responsive hydrogels. *Nature Materials, 9*, 159–164.

Kim, M., Park, K. J., Seok, S., Ok, J. M., Jung, H.-T., Choe, J., & Kim, D. H. (2015b). Fabrication of microcapsules for dye-doped polymer-dispersed liquid crystal-based smart windows. *ACS Applied Materials and Interfaces, 7*, 17904–17909.

Kim, P., Hu, Y., Alvarenga, J., Kolle, M., Suo, Z., & Aizenberg, J. (2013). Rational design of mechano-responsive optical materials by fine tuning the evolution of strain-dependent wrinkling patterns. *Advanced Optical Materials, 1*, 381–388.

Lamoureux, A., Lee, K., Shlian, M., Forrest, S. R., & Shtein, M. (2015). Dynamic kirigami structures for integrated solar tracking. *Nature Communications, 6*, 8092.

Lampert, C. M. (2004). Chromogenic smart materials. *Materials Today, 7*, 28–35.

Lee, S. G., Lee, D. Y., Lim, H. S., Lee, D. H., Lee, S., & Cho, K. (2010). Switchable transparency and wetting of elastomeric smart windows. *Advanced Materials, 22*, 5013–5017.

Lee, S. J., Ha, N., & Kim, H. (2019). Superhydrophilic-superhydrophobic water harvester inspired by wetting property of cactus stem. *ACS Sustainable Chemistry and Engineering, 7*, 10561–10569.

Lekouch, I., Muselli, M., Kabbachi, B., Ouazzani, J., Melnytchouk-Milimouk, I., & Beysens, D. (2011). Dew, fog, and rain as supplementary sources of water in south-western Morocco. *Energy, 36*, 2257–2265.

Li, H., Chen, C., Jin, J., Bi, W., Zhang, B., Chen, X., Xu, L., Liu, D., Dai, Q., & Song, H. (2018). Near-infrared and ultraviolet to visible photon conversion for full spectrum response perovskite solar cells. *Nano Energy, 50*, 699–709.

Li, J., Ran, R., Wang, H., Wang, Y., Chen, Y., Niu, S., Arratia, P. E., & Yang, S. (2021a). Aerodynamics-assisted, efficient and scalable kirigami fog collectors. *Nature Communications, 12*, 5484.

Li, Y., Zhao, Y., Chi, Y., Hong, Y., & Yin, J. (2021b). Shape-morphing materials and structures for energy-efficient building envelopes. *Materials Today Energy, 22*, 100874.

Li, M., Magdassi, S., Gao, Y., & Long, Y. (2017). Hydrothermal synthesis of VO2 polymorphs: Advantages, challenges and prospects for the application of energy efficient smart windows. *Small, 13*, 1701147.

Lin, G., Chandrasekaran, P., Lv, C., Zhang, Q., Tang, Y., Han, L., & Yin, J. (2017). Self-similar hierarchical wrinkles as a potential multifunctional smart window with simultaneously tunable transparency, structural color, and droplet transport. *ACS Applied Materials and Interfaces, 9*, 26510–26517.

Lin, G., Zhang, Q., Lv, C., Tang, Y., & Yin, J. (2018). Small degree of anisotropic wetting on self-similar hierarchical wrinkled surfaces. *Soft Matter, 14*, 1517–1529.

Llordés, A., Garcia, G., Gazquez, J., & Milliron, D. J. (2013). Tunable near-infrared and visible-light transmittance in nanocrystal-in-glass composites. *Nature, 500*, 323–326.

Macêdo, M. A., Dall'Antonia, L. H., Valla, B., & Aegerter, M. A. (1992). Electrochromic smart windows. *Journal of Non-Crystalline Solids, 147–148*, 792–798.

Madida, I. G., Simo, A., Sone, B., Maity, A., Kana Kana, J. B., Gibaud, A., Merad, G., Thema, F. T., & Maaza, M. (2014). Submicronic VO2–PVP composites coatings for smart windows applications and solar heat management. *Solar Energy, 107*, 758–769.

Matsumoto, K., Sakikawa, N., & Miyata, T. (2018). Thermo-responsive gels that absorb moisture and ooze water. *Nature Communications, 9*, 2315.

Mei, A., Li, X., Liu, L., Ku, Z., Liu, T., Rong, Y., Xu, M., Hu, M., Chen, J., Yang, Y., Grätzel, M., & Han, H. (2014). A hole-conductor–free, fully printable mesoscopic perovskite solar cell with high stability. *Science, 345*, 295–298.

Meng, Y., Li, X., Wang, S., Lau, C., Hu, H., Ke, Y., Tan, G., Yang, J., & Long, Y. (2022). Flexible smart photovoltaic foil for energy generation and conservation in buildings. *Nano Energy, 91*, 106632.

Miller, M. J., & Wang, J. (2015). Influence of grain size on transition temperature of thermochromic VO2. *Journal of Applied Physics, 117*, 034307.

Parkin, I. P., & Manning, T. D. (2006). Intelligent thermochromic windows. *Journal of Chemical Education, 83*, 393.

Pérez-Lombard, L., Ortiz, J., & Pout, C. (2008). A review on buildings energy consumption information. *Energy and Buildings, 40*, 394–398.

Piccolo, A., & Simone, F. (2015). Performance requirements for electrochromic smart window. *Journal of Building Engineering, 3*, 94–103.

Powell, D., Hischier, I., Jayathissa, P., Svetozarevic, B., & Schlüter, A. (2018). A reflective adaptive solar façade for multi-building energy and comfort management. *Energy and Buildings, 177*, 303–315.

Rauh, R. D. (1999). Electrochromic windows: An overview. *Electrochimica Acta, 44*, 3165–3176.

Reichert, S., Menges, A., & Correa, D. (2015). Meteorosensitive architecture: Biomimetic building skins based on materially embedded and hygroscopically enabled responsiveness. *Computer-Aided Design, 60*, 50–69.

Sundriyal, P., & Bhattacharya, S. (2018). Inkjet-printed sensors on flexible substrates. In S. Bhattacharya, A. K. Agarwal, N. Chanda, A. Pandey & A. K. Sen (Eds.), *Environmental, chemical and medical sensors.* Singapore: Springer Singapore.

Tällberg, R., Jelle, B. P., Loonen, R., Gao, T., & Hamdy, M. (2019). Comparison of the energy saving potential of adaptive and controllable smart windows: A state-of-the-art review and simulation studies of thermochromic, photochromic and electrochromic technologies. *Solar Energy Materials and Solar Cells, 200*, 109828.

Tang, Y., Lin, G., Yang, S., Yi, Y. K., Kamien, R. D., & Yin, J. (2017). Programmable kiri-kirigami metamaterials. *Advanced Materials, 29*, 1604262.

Thomas, A. V., Andow, B. C., Suresh, S., Eksik, O., Yin, J., Dyson, A. H., & Koratkar, N. (2015). Controlled crumpling of graphene oxide films for tunable optical transmittance. *Advanced Materials, 27*, 3256–3265.

Tomholt, L., Geletina, O., Alvarenga, J., Shneidman, A. V., Weaver, J. C., Fernandes, M. C., Mota, S. A., Bechthold, M., & Aizenberg, J. (2020). Tunable infrared transmission for energy-efficient pneumatic building façades. *Energy and Buildings, 226*, 110377.

Vergaz, R., Sánchez-Pena, J.-M., Barrios, D., Vázquez, C., & Contreras-Lallana, P. (2008). Modelling and electro-optical testing of suspended particle devices. *Solar Energy Materials and Solar Cells, 92*, 1483–1487.

Vieira, F., Sarmento, B., Reis-Machado, A. S., Facão, J., Carvalho, M. J., Mendes, M. J., Fortunato, E., & Martins, R. (2019). Prediction of sunlight-driven CO2 conversion: Producing methane from photovoltaics, and full system design for single-house application. *Materials Today Energy, 14*, 100333.

Wang, H., Yi, X., & Li, Y. (2005). Fabrication of VO2 films with low transition temperature for optical switching applications. *Optics Communications, 256*, 305–309.

Wang, J., Zhang, L., Yu, L., Jiao, Z., Xie, H., Lou, X. W., & Wei Sun, X. (2014). A bifunctional device for self-powered electrochromic window and self-rechargeable transparent battery applications. *Nature Communications, 5*, 4921.

Wang, K., Wu, H., Meng, Y., Zhang, Y., & Wei, Z. (2012). Integrated energy storage and electrochromic function in one flexible device: An energy storage smart window. *Energy and Environmental Science, 5*, 8384–8389.

Wang, L., Liu, Y., Zhan, X., Luo, D., & Sun, X. (2019a). Photochromic transparent wood for photo-switchable smart window applications. *Journal of Materials Chemistry C, 7*, 8649–8654.

Wang, N., Duchamp, M., Dunin-Borkowski, R. E., Liu, S., Zeng, X., Cao, X., & Long, Y. (2016a). Terbium-doped VO2 thin films: Reduced phase transition temperature and largely enhanced luminous transmittance. *Langmuir, 32*, 759–764.

Wang, N., Goh, Q. S., Lee, P. L., Magdassi, S., & Long, Y. (2017). One-step hydrothermal synthesis of rare earth/W-codoped VO2 nanoparticles: Reduced phase transition temperature and improved thermochromic properties. *Journal of Alloys and Compounds, 711*, 222–228.

Wang, S., Gao, W., Hu, X.-Y., Shen, Y.-Z., & Wang, L. (2019b). Supramolecular strategy for smart windows. *Chemical Communications, 55*, 4137–4149.

Wang, S., Liu, G., Hu, P., Zhou, Y., Ke, Y., Li, C., Chen, J., Cao, T., & Long, Y. (2018). Largely lowered transition temperature of a VO2/carbon hybrid phase change material with high thermal emissivity switching ability and near infrared regulations. *Advanced Materials Interfaces, 5*, 1801063.

Wang, Y., Runnerstrom, E. L., & Milliron, D. J. (2016b). Switchable materials for smart windows. *Annual Review of Chemical and Biomolecular Engineering, 7*, 283–304.

Wu, L. Y. L., Zhao, Q., Huang, H., & Lim, R. J. (2017). Sol-gel based photochromic coating for solar responsive smart window. *Surface and Coatings Technology, 320*, 601–607.

Wu, S., Zhang, Q., Deng, Y., Li, X., Luo, Z., Zheng, B., & Dong, S. (2020). Assembly pattern of supramolecular hydrogel induced by lower critical solution temperature behavior of low-molecular-weight gelator. *Journal of the American Chemical Society, 142*, 448–455.

Xie, Z., Jin, X., Chen, G., Xu, J., Chen, D., & Shen, G. (2014). Integrated smart electrochromic windows for energy saving and storage applications. *Chemical Communications, 50*, 608–610.

Xu, C., Cai, L., Zhong, M., & Zheng, S. (2015). Low-cost and rapid prototyping of microfluidic paper-based analytical devices by inkjet printing of permanent marker ink. *RSC Advances, 5*, 4770–4773.

Xu, T., Lin, Y., Zhang, M., Shi, W., & Zheng, Y. (2016). High-efficiency fog collector: water unidirectional transport on heterogeneous rough conical wires. *ACS Nano, 10*, 10681–10688.

Yang, L., Ge, D., Zhao, J., Ding, Y., Kong, X., & Li, Y. (2012). Improved electrochromic performance of ordered macroporous tungsten oxide films for IR electrochromic device. *Solar Energy Materials and Solar Cells, 100*, 251–257.

Yang, P., Sun, P., Chai, Z., Huang, L., Cai, X., Tan, S., Song, J., & Mai, W. (2014). Large-scale fabrication of pseudocapacitive glass windows that combine electrochromism and energy storage. *Angewandte Chemie International Edition, 53*, 11935–11939.

Yi, Y. K., Yin, J., & Tang, Y. (2018). Developing an advanced daylight model for building energy tool to simulate dynamic shading device. *Solar Energy, 163*, 140–149.

Yin, W.-J., Shi, T., & Yan, Y. (2014). Unusual defect physics in CH3NH3PbI3 perovskite solar cell absorber. *Applied Physics Letters, 104*, 063903.

Yu, H., Guo, J., Wang, C., Zhang, J., Liu, J., Zhong, X., Dong, G., & Diao, X. (2019). High performance in electrochromic amorphous WOx film with long-term stability and tunable switching times via Al/Li-ions intercalation/deintercalation. *Electrochimica Acta, 318*, 644–650.

Zang, J., Ryu, S., Pugno, N., Wang, Q., Tu, Q., Buehler, M. J., & Zhao, X. (2013). Multifunctionality and control of the crumpling and unfolding of large-area graphene. *Nature Materials, 12*, 321–325.

Zeng, S., Zhang, D., Huang, W., Wang, Z., Freire, S. G., Yu, X., Smith, A. T., Huang, E. Y., Nguon, H., & Sun, L. (2016). Bio-inspired sensitive and reversible mechanochromisms via strain-dependent cracks and folds. *Nature Communications, 7*, 11802.

Zhai, L., Berg, M. C., Cebeci, F. Ç., Kim, Y., Milwid, J. M., Rubner, M. F., & Cohen, R. E. (2006). Patterned superhydrophobic surfaces: Toward a synthetic mimic of the Namib desert beetle. *Nano Letters, 6*, 1213–1217.

Zhang, K., Zhang, M., Feng, X., Hempenius, M. A., & Vancso, G. J. (2017a). Switching light transmittance by responsive organometallic poly(ionic liquid)s: Control by cross talk of thermal and redox stimuli. *Advanced Functional Materials, 27*, 1702784.

Zhang, L., Zhao, Y., & Dai, Q. (2021). Recent progress in perovskite solar cell: Fabrication, Efficiency, and stability. In J. K. Roy, S. Kar, & J. Leszczynski (Eds.), *Development of solar cells: Theory and experiment.* Cham: Springer International Publishing.

Zhang, Q., Tang, Y., Hajfathalian, M., Chen, C., Turner, K. T., Dikin, D. A., Lin, G., & Yin, J. (2017b). Spontaneous periodic delamination of thin films to form crack-free metal and silicon ribbons with high stretchability. *ACS Applied Materials and Interfaces, 9*, 44938–44947.

Zhang, Q., & Yin, J. (2018). Spontaneous buckling-driven periodic delamination of thin films on soft substrates under large compression. *Journal of the Mechanics and Physics of Solids, 118*, 40–57.

Zhang, S., Cao, S., Zhang, T., & Lee, J. Y. (2020). Plasmonic oxygen-deficient TiO2-x nanocrystals for dual-band electrochromic smart windows with efficient energy recycling. *Advanced Materials, 32*, 2004686.

Zheng, S., Xu, Y., Shen, Q., & Yang, H. (2015). Preparation of thermochromic coatings and their energy saving analysis. *Solar Energy, 112*, 263–271.

Zhou, J., Gao, Y., Zhang, Z., Luo, H., Cao, C., Chen, Z., Dai, L., & Liu, X. (2013). VO2 thermochromic smart window for energy savings and generation. *Scientific Reports, 3*, 3029.

Zhou, Y., Wang, S., Peng, J., Tan, Y., Li, C., Boey, F. Y. C., & Long, Y. (2020). Liquid thermo-responsive smart window derived from hydrogel. *Joule, 4*, 2458–2474.